



Contents lists available at ScienceDirect

Probabilistic Engineering Mechanics

journal homepage: www.elsevier.com/locate/probengmech

Response spectral density determination for nonlinear systems endowed with fractional derivatives and subject to colored noise

Fan Kong^{a,b,*}, Pol D. Spanos^c^a School of Civil Engineering and Architecture, Wuhan University of Technology, 122 Luoshi Road, Wuhan, Hubei 430070, China^b George R. Brown School of Engineering, Rice University, Houston 77251, TX, USA^c George R. Brown School of Engineering, Rice University, P.O. Box 1892, Houston 77251, TX, USA

ARTICLE INFO

Keywords:

Harmonic balance
Spectral representation
Fractional derivative
Power spectral density

ABSTRACT

A computationally efficient method for determining the response of non-linear stochastic dynamic systems endowed with fractional derivative elements subject to stochastic excitation is presented. The method relies on a spectral representation both for the system excitation and its response. Specifically, first the ordinary non-linear differential equation of motion is transferred into a set of non-linear algebra equations by employing the harmonic balance method. Next, the response Fourier coefficients are determined by solving these non-linear equations. Finally, repeated use of the proposed procedure yields the response power spectral density. Pertinent numerical examples, including a fractional Duffing and a bilinear oscillator, demonstrate the accuracy of the proposed method.

1. Introduction

The determination of the stochastic response of nonlinear dynamic systems subject to external stochastic excitations remains a challenge for the reliability evaluation and risk assessment of engineering systems [1]. Appropriate modeling of the system dynamic characteristics not only improves the model accuracy, but may also simplify the methods adopted for stochastic dynamic analysis. As far as viscoelasticity modeling in engineering application is concerned, the fractional derivative concept has been extensively used in structural control [2]; consider the structural base isolation [3] for instance. An advantage of the fractional modeling for the viscoelastic behavior lies in its compact form. That is, compared to the classic standard mechanical models (SMMs, series and/or parallel connection of dampers and springs), fractional model needs fewer parameters to capture the time-domain (creep and stress relaxation), and frequency-domain (loss and storage modulus) material functions accurately and simultaneously [4]. In this regard, it may be argued that modeling by fractional derivatives simplifies the methods adopted for system stochastic behavior prediction.

This paper focuses on the stochastic response spectrum determination of non-linear dynamic systems endowed with fractional elements. Research on this theme is relatively limited compared to its deterministic and/or linear counterparts. Specifically, for the fractional deterministic linear response, Fourier transform [5], Laplace transform [6], and the eigenvector expansion method [7,8] can be used for obtaining analytical solutions under certain conditions. While on the other hand,

for the fractional stochastic linear systems, it was proved in Ref. [9] that in the frequency domain the response power spectral density (PSD) can be determined by a standard procedure for integral-order derivatives systems. As far as the time-domain solution is concerned, often the double integration of the fractional impulse response function [10–12] can be used, limiting its application only to systems with a few DOFs. Study on the stochastic analysis of non-linear fractional system mainly focuses on the extension of the classic stochastic method for integral-order systems, including stochastic averaging, statistical linearization, and path integral [13–17]. Similarly to their integral-order counterpart, the applicability of these methods is usually problem dependent.

Undoubtedly, the most versatile method for stochastic system analysis is the Monte Carlo simulation (MCS) [18]. This sampling-experiment method, although quite time-consuming, for large-scale engineering problems becomes increasingly important with the advent of modern computational efficiency. Within this framework, several step-by-step integration methods have been developed for determining sample responses of fractional systems [19]. They are named after the schemes for discretizing the fractional and the integral-order derivatives [20]. For instance, the numerical method developed in Ref. [15] is, in fact, a GL (Grünwal–Letnikov) based Newmark- β scheme; also see [20]. However, there are limitations to apply the time domain MCS for fractional stochastic dynamic systems. Specifically, first weighting parameters of all of the past steps should be updated, which may lead to a significant increase in computational cost [3,15,20]. Besides, the duration of the

* Corresponding author.

E-mail addresses: kongfan@whut.edu.cn (F. Kong), spanos@rice.edu (P.D. Spanos).

equally spaced time step should be short enough to capture the high-frequency content induced by the non-linear effect [21], and thus, more discrete time steps are needed for a fixed time duration. In this context, it may be argued that the time-domain MCS is not computationally efficient for non-linear fractional systems, at least when compared to their integer-order counterpart.

To address this problem, the paper presents a frequency-domain MCS method for the response spectral density determination of non-linear fractional systems subject to stochastic excitations. For this purpose, following the procedure adopted by [21] and relying on the spectral representation for the excitation and response, the multi-harmonic balance method is utilized to recast the nonlinear fractional order differential equation into a set of non-linear algebraic equations with unknown response Fourier coefficients. These equations can be solved readily by established numerical methods. Next, response spectral characteristics can be estimated by repeated use of the proposed method. Finally, numerical examples including a Duffing and a bilinear oscillator demonstrates the accuracy of the proposed method.

2. Discrete spectral representation of stochastic processes

The spectral representation method for stochastic processes can be regarded as a stochastic extension of Fourier series of a deterministic process. The method decomposes a stochastic signal into a summation of an infinite number of harmonics weighting by random variables. Specifically, a stationary stochastic process $X(t)$, $-\infty < t < \infty$ in the wide sense with non-zero mean value and two-sided power spectral density (PSD) $S_X(\omega)$, can be approximately simulated as a random combination of N -harmonics [22]

$$X(t) \approx c_0 + \sqrt{2} \sum_{n=1}^N M_n \cos(\omega_n t + \Phi_n), \quad (1)$$

where c_0 is the deterministic mean value; $M_n = [2S_X(\omega_n) \Delta\omega]^{1/2}$ is the harmonic amplitudes; $\omega_n = n\Delta\omega$ is the discrete frequencies and $\Delta\omega = \omega_u/N$ is the frequency sampling space; $T_0 = 2\pi/\Delta\omega$ is the fundamental period; and ω_u is the cutoff frequency beyond which the PSD $S_X(\omega)$ can be assumed to be zero. The randomness of the process is derived from the independent random phases Φ_n s which are uniformly distributed in the interval $[0, 2\pi]$. Further, it can be argued that when $N \rightarrow \infty$, and $\Delta\omega$ is sufficiently small, a stochastic process can be adequately represented by Eq. (1) [22]. In this case, the expression captures, in fact, a fundamental theorem proposed by Cramer [23] regarding stationary stochastic process representation via two mutually incremental orthogonal processes. Further expansion of Eq. (1) leads to

$$X(t) \approx c_0 + \sum_{n=1}^N (C_n \cos \omega_n t + D_n \sin \omega_n t), \quad (2)$$

where

$$C_n = \sqrt{2} M_n \cos \Phi_n = 2 [S_X(\omega_n) \Delta\omega]^{1/2} \cos \Phi_n, \quad (3)$$

$(n = 1, 2, \dots, N),$

$$D_n = -\sqrt{2} M_n \sin \Phi_n = -2 [S_X(\omega_n) \Delta\omega]^{1/2} \sin \Phi_n, \quad (4)$$

$(n = 1, 2, \dots, N).$

It can be proved that C_n s and D_n s are independent random variables with

$$E[C_n] = E[D_n] = 0, \quad (5)$$

$$E[C_n^2] = E[D_n^2] = 2S_X(\omega_n) \Delta\omega, \quad (6)$$

$$E[C_n C_m] = E[D_n D_m] = 0 \text{ for } n \neq m, \quad (7)$$

and

$$E[C_n D_m] = 0 \text{ for any } n \text{ and } m \quad (8)$$

3. Harmonic balance solution of non-linear fractional systems

Next, consider a non-linear stochastic dynamic system endowed with fractional derivative term governed by the equation

$$m\ddot{X}(t) + cD_c^q[X(t)] + kX(t) + \lambda kG(X, \dot{X}) = F(t), \quad (9)$$

where $m, c = 2\zeta_0 m \omega_n^{2-q}$ and k are the mass, damping and stiffness of the system, respectively; q represents the order of fractional derivative; $\omega_n = \sqrt{k/m}$ is the corresponding natural frequency; λ denotes a parameter quantifying the non-linear intensity; the symbol “D” with the subscript “c” denotes the fractional derivative of the system response $x(t)$ in the Caputo’s sense; $G(X, \dot{X})$ is the non-linear component in terms of displacement and velocity; and $F(t)$ is a stochastic excitation with PSD $S_F(\omega)$. For further elucidation of the fractional derivative concept, one may be found further in [24].

Similarly, the stochastic excitation process can be approximately simulated by the spectral representation with a finite number of harmonics shown in Eq. (2). That is,

$$F(t) \approx a_0 + \sum_{n=1}^N A_n \cos \omega_n t + B_n \sin \omega_n t, \quad (10)$$

where A_n s and B_n s are independent random variables with the same properties shown in Eqs. (5)–(8).

3.1. Formulation

Taking the second derivative of Eq. (2) leads to

$$\ddot{X}(t) = \sum_{n=1}^N (-\omega_n^2 C_n \cos \omega_n t - \omega_n^2 D_n \sin \omega_n t). \quad (11)$$

Further, the fractional derivatives of the response can be written as [25]

$$D_c^q[X(t)] = \frac{c_0}{\Gamma(1-q)t^q} + \sum_{n=1}^N \left[C_n \omega_n^q \cos\left(\omega_n t + \frac{\pi}{2} q\right) + D_n \omega_n^q \sin\left(\omega_n t + \frac{\pi}{2} q\right) \right]. \quad (12)$$

Different from the integer derivatives of a constant, the fractional derivative of c_0 in the Caputo’s sense does not equal zero. Substituting Eqs. (11)–(12) into Eq. (9) yields Eq. (13) which is given in [Box I](#). Proceeding next to multi-harmonic balance on both sides of Eq., yields the set of $(2N+1)$ algebraic equations (14)–(16) which are given in [Box II](#). Clearly, the unknown response Fourier coefficients ($c_0, C_1, D_1, C_2, D_2, \dots, C_N, D_N$) can be obtained by solving the above set of algebraic equations by established numerical methods.

3.2. Solution via Newton’s iterative method

Eqs. (14)–(16) are a set of coupled non-linear algebraic equations with unknown response Fourier coefficients that can be readily solved by numerical methods. Newton’s iterative method is adopted herein. In this regard, one need to solve the following matrix equation for obtaining the unknown quantities at the i th step. That is,

$$\mathbf{K}(\boldsymbol{\alpha}^{(i)}) + \mathbf{J}(\boldsymbol{\alpha}^{(i)}) (\boldsymbol{\alpha}^{(i+1)} - \boldsymbol{\alpha}^{(i)}) = \mathbf{0}. \quad (17)$$

According to Eqs. (14)–(16), the column vector \mathbf{K} with $2N+1$ entries can be written as Eqs. (18)–(20) which are given in [Box III](#). Further, the $(2N+1) \times (2N+1)$ entries of the Jacobian matrix $\mathbf{J} = \partial \mathbf{K} / \partial \boldsymbol{\alpha}$ are Eqs. (21)–(23) which are given in [Box IV](#) where $\boldsymbol{\alpha} = [c_0, C_1, D_1, C_2, D_2, \dots, C_N, D_N]^T$ is a column vector with entries being unknown response Fourier coefficients; δ denotes the Kronecker delta. Regarding the numerical implementation of the proposed method, some comments are in order. First, the Fourier integrations of the non-linear terms in Eqs. (19)–(23) must be appropriately determined. This can be achieved by resorting to the celebrated Fast Fourier Transform (FFT), which may produce the

$$m \sum_{n=1}^N (-\omega_n^2 C_n \cos \omega_n t - D_n \omega_n^2 \sin \omega_n t) + c \left\{ \frac{c_0}{\Gamma(1-q)t^q} + \sum_{n=1}^N \left[C_n \omega_n^q \cos \left(\omega_n t + \frac{\pi}{2} q \right) + D_n \omega_n^q \sin \left(\omega_n t + \frac{\pi}{2} q \right) \right] \right\} + k \left\{ c_0 + \sum_{n=1}^N (C_n \cos \omega_n t + D_n \sin \omega_n t) \right\} + \lambda k G(X, \dot{X}) = a_0 + \sum_{n=1}^N (A_n \cos \omega_n t + B_n \sin \omega_n t) \tag{13}$$

Box I.

$$kc_0 + \frac{cc_0}{T_0 \Gamma(1-q)} \int_0^{T_0} t^{-q} dt + \frac{\lambda k}{T_0} \int_0^{T_0} G(X, \dot{X}) dt = A_0, \tag{14}$$

$$(k - m\omega_n^2) C_n + c\omega_n^q \left(C_n \cos \frac{\pi q}{2} + D_n \sin \frac{\pi q}{2} \right) + \frac{2cc_0}{T_0 \Gamma(1-q)} \int_0^{T_0} t^{-q} \cos \omega_n t dt + \frac{2\lambda k}{T_0} \int_0^{T_0} G(X, \dot{X}) \cos \omega_n t dt = A_n, \quad (n = 1, 2, \dots, N), \tag{15}$$

$$(k - m\omega_n^2) D_n + c\omega_n^q \left(-C_n \sin \frac{\pi q}{2} + D_n \cos \frac{\pi q}{2} \right) + \frac{2cc_0}{T_0 \Gamma(1-q)} \int_0^{T_0} t^{-q} \sin \omega_n t dt + \frac{2\lambda k}{T_0} \int_0^{T_0} G(X, \dot{X}) \sin \omega_n t dt = B_n, \quad (n = 1, 2, \dots, N). \tag{16}$$

Box II.

$$K_1(\boldsymbol{\alpha}) = \frac{\lambda k}{T_0} \int_0^{T_0} G(X, \dot{X}) dt + kc_0 + \frac{cc_0}{T_0 \Gamma(1-q)} \int_0^{T_0} t^{-q} dt - a_0, \tag{18}$$

$$K_{2n}(\boldsymbol{\alpha}) = (-m\omega_n^2 + c\omega_n^q \cos \frac{\pi q}{2} + k) \alpha_{2n} + (c\omega_n^q \sin \frac{\pi q}{2}) \alpha_{2n+1} + \frac{2cc_0}{T_0 \Gamma(1-q)} \int_0^{T_0} t^{-q} \cos \omega_n t dt + \frac{2\lambda k}{T_0} \int_0^{T_0} G(X, \dot{X}) \cos \omega_n t dt - A_n, \tag{19}$$

$(n = 1, 2, \dots, N),$

$$K_{2n+1}(\boldsymbol{\alpha}) = (-m\omega_n^2 + c\omega_n^q \cos \frac{\pi q}{2} + k) \alpha_{2n+1} - (c\omega_n^q \sin \frac{\pi q}{2}) \alpha_{2n} + \frac{2cc_0}{T_0 \Gamma(1-q)} \int_0^{T_0} t^{-q} \sin \omega_n t dt + \frac{2\lambda k}{T_0} \int_0^{T_0} G(X, \dot{X}) \sin \omega_n t dt - B_n, \tag{20}$$

$(n = 1, 2, \dots, N).$

Box III.

$$J_{1,j} = \frac{\lambda k}{T_0} \int_0^{T_0} \left(\frac{\partial G}{\partial X} \frac{\partial X}{\partial \alpha_j} + \frac{\partial G}{\partial \dot{X}} \frac{\partial \dot{X}}{\partial \alpha_j} \right) dt + \left(k + \frac{c \int_0^{T_0} t^{-q} dt}{T_0 \Gamma(1-q)} \right) \delta_{1,j}, \quad (j = 1, 2, \dots, 2N + 1), \tag{21}$$

$$J_{2n,j} = (-m\omega_n^2 + c\omega_n^q \cos \frac{\pi q}{2} + k) \delta_{j/2,n} + (c\omega_n^q \sin \frac{\pi q}{2}) \delta_{(j-1)/2,n} + \frac{2\lambda k}{T_0} \int_0^{T_0} \left(\frac{\partial G}{\partial X} \frac{\partial X}{\partial \alpha_j} + \frac{\partial G}{\partial \dot{X}} \frac{\partial \dot{X}}{\partial \alpha_j} \right) \cos \omega_n t dt, \tag{22}$$

$(n = 1, 2, \dots, N; j = 1, 2, \dots, 2N + 1),$

and

$$J_{2n+1,j} = (-c\omega_n^q \sin \frac{\pi q}{2}) \delta_{j/2,n} + (-m\omega_n^2 + c\omega_n^q \cos \frac{\pi q}{2} + k) \delta_{(j-1)/2,n} + \frac{2\lambda k}{T_0} \int_0^{T_0} \left(\frac{\partial G}{\partial X} \frac{\partial X}{\partial \alpha_j} + \frac{\partial G}{\partial \dot{X}} \frac{\partial \dot{X}}{\partial \alpha_j} \right) \sin \omega_n t dt, \tag{23}$$

$(n = 1, 2, \dots, N; j = 1, 2, \dots, 2N + 1),$

Box IV.

so-called aliasing effect. This effect can be circumvented numerically by padding requisite zeros to the response Fourier coefficients $\boldsymbol{\alpha}$ [21,26], but this procedure increases significantly the requisite computational cost. A better choice which not only circumvents the aliasing effect, but it also improves computational efficiency is the closed form solution for the Fourier integrals of polynomial non-linearities [21]. Second, as far as arbitrary nonlinearity is concerned, the proposed method can be applied to an equivalent cubic polynomial whose coefficients are determined by a least square fitting method on the period $[0, T_0]$. Next, the first term on the right side of Eq. (12) derived from the fractional derivative of the response mean value c_0 , barely increases the computational time of Newton's iteration procedure. This is due

to the fact that the term does not include any unknown entry of $\boldsymbol{\alpha}$ and only contributes to very low-frequency content.

4. Numerical examples

4.1. Duffing oscillator application

To assess the usefulness of the proposed method for the response determination of stochastic dynamic systems, a fractional Duffing oscillator

$$m\ddot{X}(t) + cD_c^q[X(t)] + kX(t) + \lambda kX^3 = F(t) \tag{24}$$

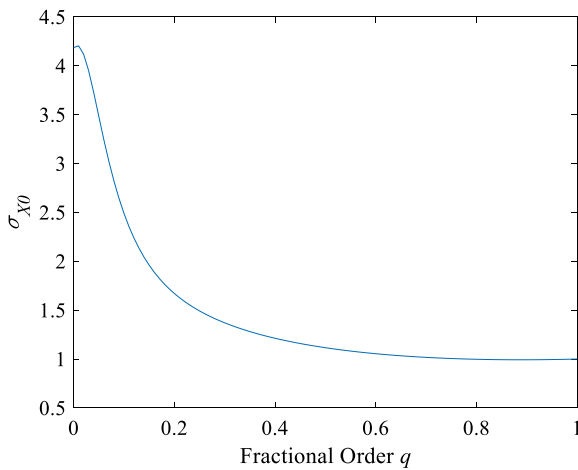


Fig. 1. Variation of the response standard deviation σ_{X_0} of the normalized linear system with fractional order q .

with a non-linear polynomial term

$$G(X, \dot{X}) = X^3 \quad (25)$$

is next considered. As an illustrative case, a stochastic excitation with invariable PSD is investigated first. Specifically, consider the equation of motion with normalized parameters

$$\ddot{X}(\tau) + 2\zeta D_c^q [X(\tau)] + X(\tau) + \lambda X^3 = F_n(\tau), \quad (26)$$

where $F_n(\tau) = F(\tau/\omega_n) / (\omega_n^2 \sigma_{X_0})$ is white noise with $S_F(\omega) = S_0$; σ_{X_0} is the displacement standard derivation of the fractional linear oscillator corresponding to Eq. (24). It can be proved that for the integer-order non-normalized linear oscillator (i.e., setting $\lambda = 0, q = 1$ in Eq. (24)) the standard deviation $\sigma_{X_0} = (\pi S_0 / (2\zeta \omega_n^3))^{1/2}$. Fig. 1 shows the variation of σ_{X_0} calculated by the numerical integration of the displacement PSD versus the fractional order q .

Considering the system parameters $\zeta = 0.2$ and $\lambda = 1$, a representative displacement time history and the corresponding Fourier amplitude spectrum calculated by the proposed method are shown in Fig. 2. For the numerical application of the proposed method, the considered frequency domain $[0, 10]$ rad/s is divided into equally spaced intervals with $\Delta\omega = 0.1$. The linear response of the fractional Duffing oscillator subject to the same excitation when $\lambda = 0$ is also plotted to indicate the nonlinear effect. It is seen from Fig. 2(a) that the time histories obtained by the proposed method and the L1 algorithm [3] agree well with each other, except at the beginning of the response due to the neglect of the initial conditions. Further, the significant difference between the linear and the nonlinear response shows that the non-linearity represented by $\lambda = 1$ is quite large. Fig. 2(b) shows the non-linearity has the effect of shifting the response Fourier spectrum to the right side of the frequency axis.

The proposed method can be used for response PSD determination by repeatedly calculating the response Fourier coefficients of samples excitations. For the present example, the response PSD is estimated over 100 realizations of response Fourier coefficients. An ensemble with the same number of response samples determined by the non-linear L1 algorithm in the time domain is also utilized to estimate response PSD. A short time step $\Delta t = 0.02$ is used in the non-linear L1 algorithm to avoid the possible aliasing effect induced by the non-linearity. Further, the statistical linearization (SL) method for fractional non-linear systems developed by Spanos and Evangelatos [27] is used for demonstrating the accuracy and efficiency of the proposed method. Specifically, for the fractional SL method, consider a non-linear system

$$m\ddot{X}(t) + cD_c^q [X(t)] + g(t) = F(t), \quad (27)$$

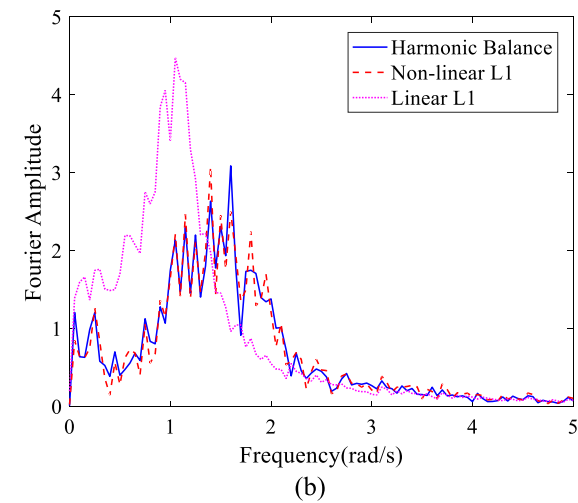
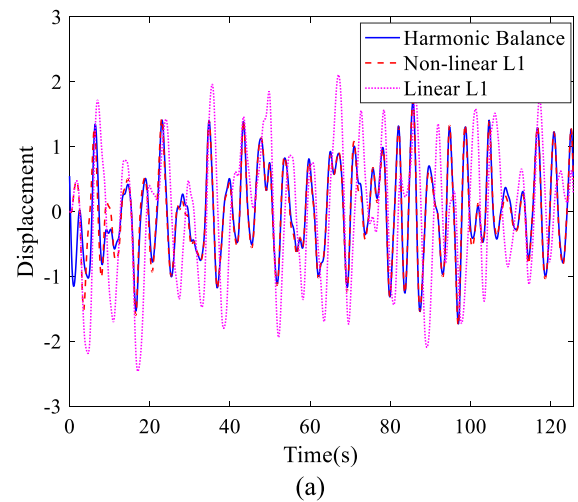


Fig. 2. (a) Response time history and (b) the corresponding Fourier amplitude spectrum of a Duffing oscillator subject to a sample of white noise when $\lambda = 1$.

where $g(t) = k[x + \lambda G(x)]$ denotes the non-linear restoring force; $G(x) = \sum_{\text{odd } l} b_l x^l$ is a non-linear function including only odd polynomial of response $x(t)$; for the non-linearity of the Duffing kind in this case $l = 3$. The response PSD can be determined by solving the equations

$$S_X(\omega) = |H(\omega)|^2 S_F(\omega) k_{\text{eq}} = k \left(1 + \lambda \sum_{\text{odd } l} l b_l A_l \right), \quad (28)$$

where $H(\omega)$ is the frequency response function of the equivalent linear system written as

$$H(\omega) = \frac{1}{-m\omega^2 + k_{\text{eq}} + c(i\omega)^q}, \quad (29)$$

and k_{eq} denotes the equivalent stiffness coefficient; A_l is the l th response moment

$$A_l = \frac{1}{\pi^{1/2}} \left(\sqrt{2} \sigma_x \right)^{l-1} \Gamma\left(\frac{l}{2}\right). \quad (30)$$

Fig. 3 shows the two-sided response PSD obtained by the three methods with four different values of λ . It is seen from all the figures that the response PSDs calculated by the proposed method agrees well with the ones calculated by the time-domain MC simulation quite well. From Fig. 3(a)–(b) one may observe that the SL slightly underestimates the dominant frequency when the λ is comparatively small. From Fig. 3(c)–(d) it is observed that the statistical linearization method

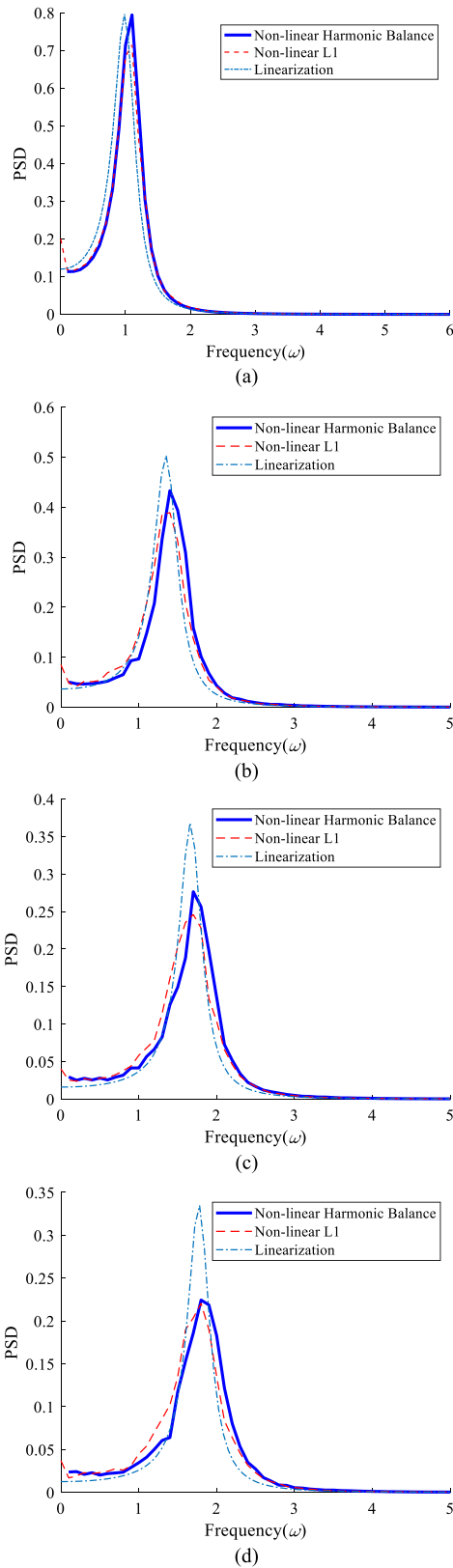


Fig. 3. Response PSD of the Duffing oscillator subject to white noise obtained by repeated use of the proposed method, the time-domain Monte Carlo simulation and the statistical linearization when (a) $\lambda = 0.01$, (b) $\lambda = 0.5$ (c) $\lambda = 1.5$ and (d) $\lambda = 2$.

yields response PSDs with higher amplitudes than the other two methods as increasing non-linearity λ . Further, the value of the dominant

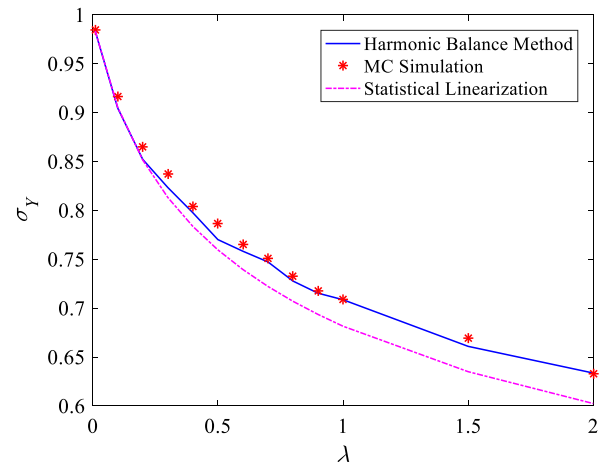


Fig. 4. Normalized displacement standard deviation σ_y versus the nonlinearity strength λ .

frequency increases, and the related spectral content becomes wider with increasing λ . This feature was observed and explained from an alternative perspective by Spanos, Kougioumtzoglou and et al. [27] in the context of the integer-order Duffing oscillator. Fig. 4 provides a comparison of the response standard deviation calculated by the proposed method, the MC simulation, and the statistical linearization, respectively, at different values of λ . It is seen that the proposed method agrees with time domain MCS quite well for all situations.

To further examine the applicability of the proposed method for the Duffing oscillator subject to colored noise, consider a stochastic excitation with the two-sided spectrum

$$S_F(\omega) = S_0 \frac{4\zeta_g^2 \omega_g^2 \omega^2}{(\omega_g^2 - \omega^2)^2 + 4\zeta_g^2 \omega_g^2 \omega^2}, \quad (31)$$

where $\zeta_g = 0.1$ and $\omega_g = 4$ rad/s relates to the damping and stiffness of a pre-filter; $S_0 = 1$ is the white noise PSD strength. The parameters related to the oscillator are chosen as $m = 1, \zeta_0 = 0.2, \omega_n = 1$ and $q = 0.75$. Similar results as in the white noise case are observed, regarding the representative non-linear sample displacements obtained by the proposed method and the non-linear L1 algorithms. Further, the considerable difference between a sample non-linear response and the corresponding linear response (when $\lambda = 5$) supports the applicability of the proposed method in treating oscillators with strong non-linearities subject to colored noise. It is worth mentioning that the convergence rate of the Newton's algorithm is quite fast for a typical sample that four to five iterations are enough to obtain a convergent result. To investigate the applicability of the proposed method in predicting response PSD of the Duffing oscillator subject to stochastic excitation with colored spectrum, the response Fourier coefficients of 100 samples are used. Fig. 5(a) – (d) shows the response PSD of the oscillator obtained by the proposed method, the time domain MCS and the statistical linearization with different values of λ . It is seen that the results obtained by the proposed method agree well the ones estimated by the MCS, whereas the statistical linearization underestimates the first dominant frequency. Spectral broadening as increasing non-linearity is also observed in this numerical case.

Fig. 6 shows a comparison of the σ_X - λ curve calculated by the proposed method and the Monte Carlo simulation. Similar to the previous white noise case, the proposed method agrees with the MC simulation quite well.

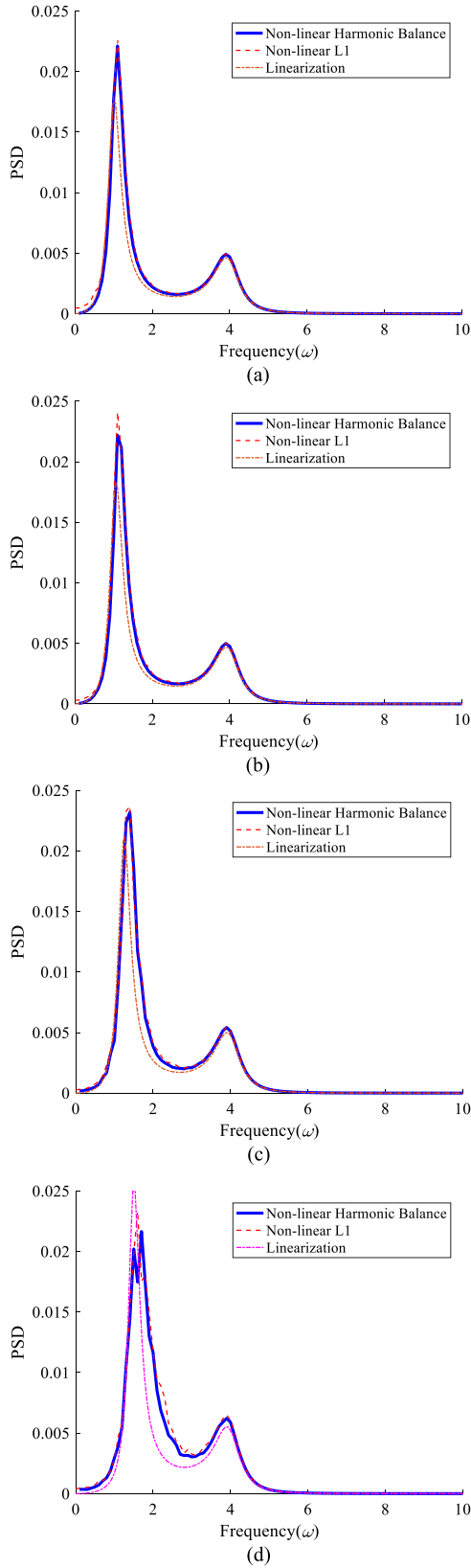


Fig. 5. Response PSD obtained by repeated use of the proposed method, the time-domain Monte Carlo simulation and the statistical linearization when (a) $\lambda = 0.01$, (b) $\lambda = 1$, (c) $\lambda = 5$ and (d) $\lambda = 10$.

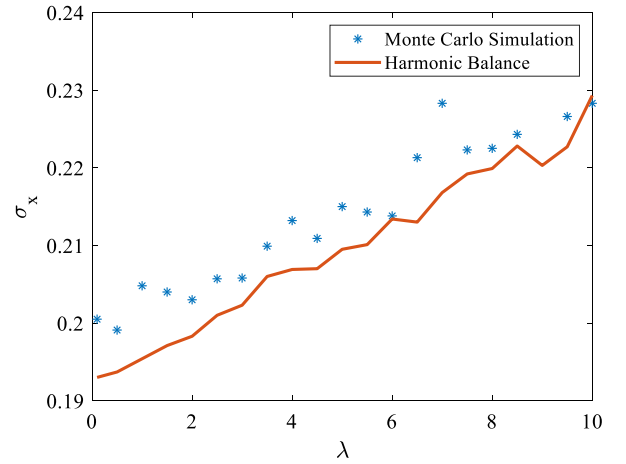


Fig. 6. Variation of the displacement standard deviation σ_x versus the nonlinearity strength λ of a fractional Duffing oscillator subject to a colored noise.

4.2. Bilinear oscillator application

To show the applicability of the proposed method to other nonlinear systems, the bilinear oscillator

$$m\ddot{X}(t) + cD_c^q[X(t)] + kX(t) + \lambda kG(X) = F(t), \quad (32)$$

where

$$G(X) = \gamma_1 X + (\gamma_2 - \gamma_1)(X - \text{sgn}(X)a)U(|X| - a) \quad (33)$$

is used as an example. Further, the coefficients $\gamma_1 = k_1/k$ and $\gamma_2 = k_2/k$ are the pre- and post-stiffness ratio of the bilinear characteristic, respectively; $\text{sgn}(\cdot)$ is the symbolic function; $U(\cdot)$ is the unit step function; λ is a constant denoting the strength of the bilinear non-linearity and a is the critical displacement at which the yield occurs. Eq. (32) can be normalized by setting $y = x/a$ and $\tau = \omega_n t$. That is,

$$\ddot{y}(\tau) + 2\zeta_0 D_c^q[y(\tau)] + y + \lambda G[y(\tau)] = F_n(\tau), \quad (34)$$

where

$$G(y) = \gamma_1 y + (\gamma_2 - \gamma_1)[y - \text{sgn}(y)]U[|y| - 1] \quad (35)$$

and

$$F_n(\tau) = \frac{F(t)}{a\omega_n^2}. \quad (36)$$

Further, the parameters are chosen as $m = 1$, $\zeta_0 = 0.2$, $\omega_n = \omega_1 = 1$ and $\omega_2 = \sqrt{2}\omega_1$, where $\omega_n = \sqrt{k/m}$, $\omega_1 = \sqrt{k_1/m}$, $\omega_2 = \sqrt{k_2/m}$, and $\zeta_0 = c/(2m\omega_n^q)$. The yield displacement a is chosen as the response standard deviation σ_{x_0} of the corresponding fractional linear system response subject to $F(t)$. Therefore, for the normalized system with weak nonlinearity, both the response standard deviation and the switch displacement equal to 1.

The polynomial fitting technique is adopted herein to make feasible to apply the multi-harmonic balance method described in Section 3 for arbitrary nonlinearities. For this purpose, the bilinear characteristic shown in Eq. (35) can be replaced by a complete cubic polynomial of X . That is

$$G(X) = [\gamma_1 X + (\gamma_2 - \gamma_1)(X - \text{sgn}(X)a)U(|X| - a)] = c_0 + c_e X + c_1 X^2 + c_4 X^3, \quad (37)$$

where c_0, c_e, c_1, c_4 are the polynomial coefficients for the generic polynomial nonlinearity; see also Ref. [21] for details. Note that the response mean value of the antisymmetric bi-linear oscillator equals to zero. For this case, although it is not necessary to incorporate c_0 and $c_1 X^2$ in the fitting polynomial, they are included herein explicitly for

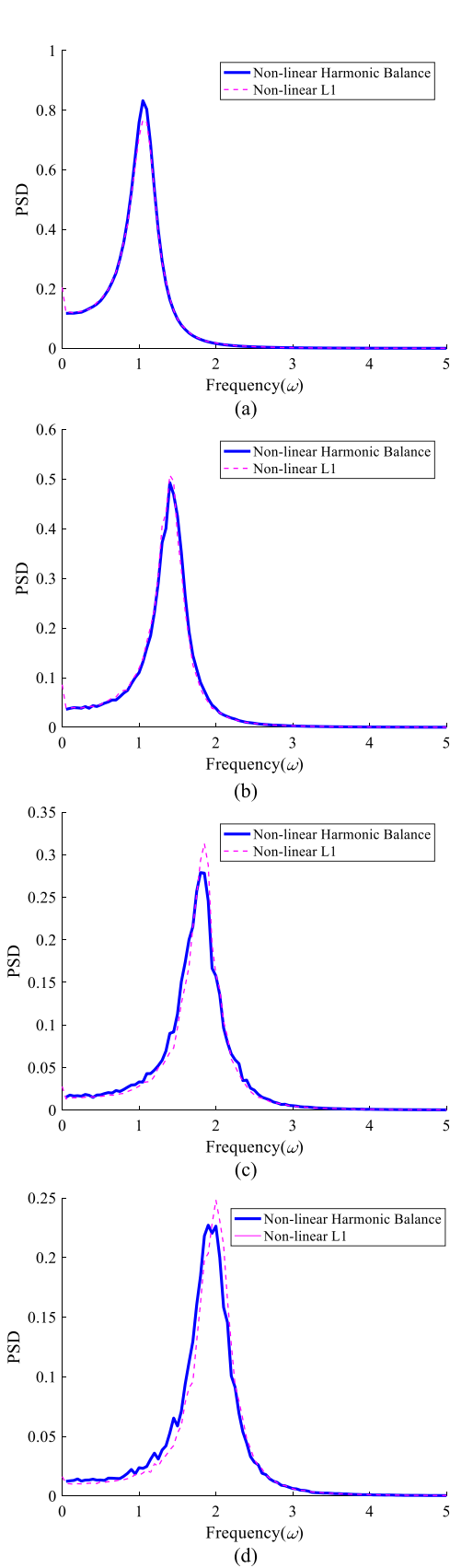


Fig. 7. Response PSD of the bilinear oscillator subject to a white noise obtained by repeated use of the proposed method and by the time-domain Monte Carlo simulation when (a) $\lambda = 0.01$, (b) $\lambda = 0.5$ (c) $\lambda = 1.5$ and (d) $\lambda = 2$.

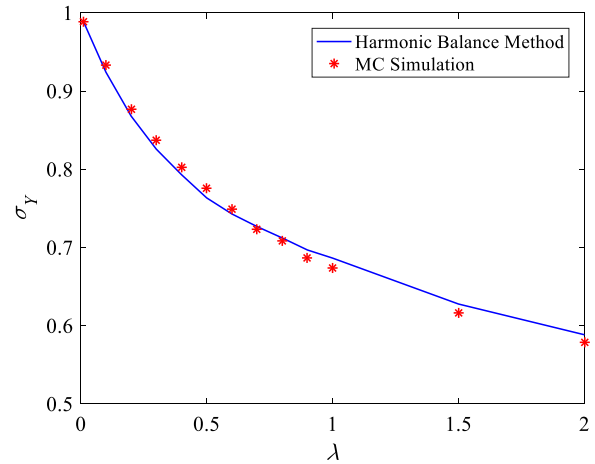


Fig. 8. Variation of the nonlinearity strength λ with the normalized displacement standard deviation σ_γ of a normalized bilinear system subject to white noise.

the general nonlinear systems. Therefore, at each step of the Newton's method, the polynomial coefficients need to be updated via the mean-square error minimization criterion on the time interval under consideration

$$\min_{c_e, c_j} \int_0^{T_0} [(c_0 + c_e X + c_1 X^2 + c_4 X^3) - G(X)]^2 dt. \quad (38)$$

The preceding equation yields a set of algebraic equations

$$\begin{bmatrix} a_{11} & a_{12} & a_{13} & a_{14} \\ - & a_{22} & a_{23} & a_{24} \\ - & - & a_{33} & a_{34} \\ - & - & - & a_{44} \end{bmatrix} \begin{Bmatrix} c_0 \\ c_e \\ c_1 \\ c_4 \end{Bmatrix} = \begin{Bmatrix} b_1 \\ b_2 \\ b_3 \\ b_4 \end{Bmatrix}, \quad (39)$$

where the entries in the symmetrical coefficient matrix are

$$a_{jl} = \frac{1}{T_0} \int_0^{T_0} X^{j+l-2} dt, j, l = 1, 2, 3, 4. \quad (40)$$

Further, b_j s are

$$b_j = \frac{1}{T_0} \int_0^{T_0} \lambda G(X) X^{j-1} dt, j = 1, 2, 3, 4. \quad (41)$$

Eq. (40) can be evaluated exactly, since the integrand function is a product of harmonics. Eq. (41) can be calculated using a standard trapezoidal rule.

Consider first the situation with the white noise excitation. In the numerical implementation of the proposed method, the frequency interval under consideration is divided into equally spaced sub-intervals with $\Delta\omega = 0.1$ rad/s. The simulated record is obtained by a modified nonlinear L1 algorithm where an iterative technique is used to locate the time instant of the stiffness switching. Fig. 7(a)–(d) illustrate the results pertaining to the two-sided PSD of the displacement obtained by the two method at different values of λ . The proposed method and the time-domain MCS, both performed over 100 sample response, yield close results. Further, Fig. 7(a)–(d) show that the PSDs become flatter with abundant frequency content as increasing non-linear strength. A good agreement between the proposed method and the MC simulation in terms of displacement standard deviation is observed in Fig. 8, where σ_γ decreases with increasing λ . As in the case of a Duffing oscillator, it is found that the proposed method is more efficient than the time-domain simulation.

Consider last a numerical example of the bilinear oscillator subject to colored noise. The oscillator parameters are chosen to be the same as in the preceding example subject to white noise. The colored noise with the two-sided spectrum shown in Eq. (31) is utilized for illustration. Figs. 9 and 10 show the comparisons of response PSDs and standard

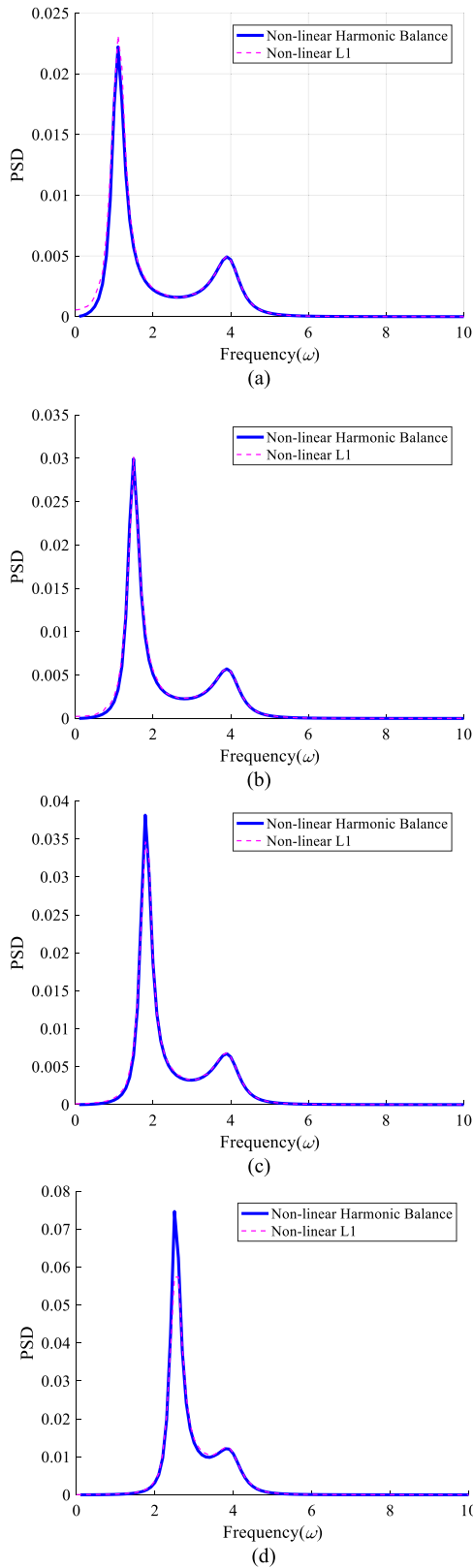


Fig. 9. Response PSD obtained by the repeated use of the proposed method and by the time-domain MCS when (a) $\lambda = 0.01$, (b) $\lambda = 1$, (c) $\lambda = 2$ and (d) $\lambda = 5$.

deviations obtained by the two methods, both performed over 100 samples, at different values of λ , respectively. Similarly, it is observed from all the figures that the proposed method exhibits reasonable

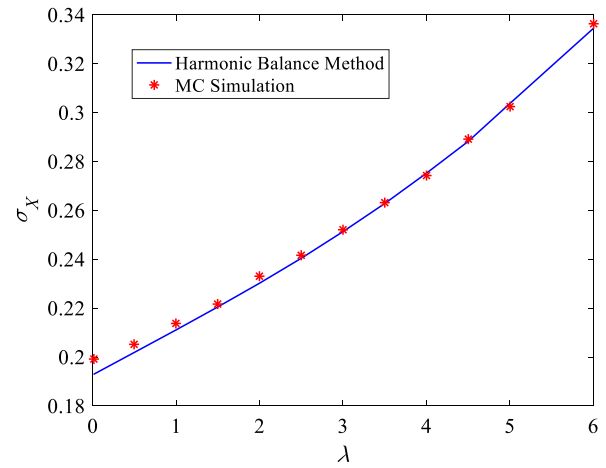


Fig. 10. Displacement standard deviation σ_x of the bilinear system subject to a colored noise versus the nonlinearity strength λ .

accuracy comparing to the related simulation results. Note that the growing nonlinear strength induces a shift of the first frequency but has no effect on the second dominant frequency.

5. Concluding remarks

A spectral representation method for determining the spectral density of the stochastic response of the non-linear systems endowed with fractional derivative terms has been proposed. For this purpose, a spectral approximation for the response/excitation, and the harmonic balance method has been used to derive a set of non-linear algebraic equations for the coefficients of the spectral representation. Oscillators with cubic and bi-linear nonlinearity have been considered as examples to demonstrate the usefulness of the proposed method for sample response. The proposed method provides an alternative highly efficient frequency-domain procedure in the framework of MCS of the response PSD for fractional non-linear systems.

An extension of the proposed method may include application to multi-degree-of-freedom or/and hysteresis systems. Further, considering the time-frequency joint resolution of wavelets, another extension of the method to treat to the full non-stationary system response using wavelet-Galerkin based representations can be pursued.

Nomenclature

A_n, B_n	= stochastic Fourier coefficients of the n th harmonic component of $F(t)$
C_n, D_n, C_m, D_m	= stochastic Fourier coefficients of the n th harmonic component of $X(t)$
D_c^q	= fractional derivative of order q in the Caputo's sense
$F(t)$	= stochastic excitation
$F_n(\tau)$	= normalized stochastic excitation
$G(\cdot)$	= non-linear restoring force of the dynamic system
$H(\omega)$	= frequency response function of a equivalent linear system
\mathbf{J}	= $(2N + 1) \times (2N + 1)$ Jacobian matrix
\mathbf{K}	= matrix equations ($(2N + 1) \times 1$ column)
M_n	= amplitude of the n th harmonic in spectral representation
N	= number of harmonic used in spectral representation

S_0	= power spectral density of white noise
T_0	= time duration of the stochastic excitation/response under consideration
$U(\cdot)$	= unit step function
$X(t)$	= stationary stochastic response
$\ddot{X}(t)$	= second derivative of $X(t)$
a	= yield displacement of the bilinear characteristic
a_0	= mean value of $F(t)$
b_l	= coefficient of the polynomial expansion of non-linear stiffness
\hat{c}, c_e, c_1, c_4	= polynomial coefficients for the generic nonlinearity
c	= damping coefficient of a dynamic system
c_0	= mean value of $X(t)$
$g(t)$	= restoring force
i	= imaginary unit
k, k_{eq}, k_1, k_2	= stiffness, equivalent stiffness, pre- and post-yield stiffness
m	= mass
$\text{sgn}(\cdot)$	= symbolic function
$y(\tau)$	= normalized response
$\Gamma(\cdot)$	= Gamma function
$\Delta\omega$	= sampling frequency step
Φ_n	= phase of the n th harmonic component
α	= column vector $[c_0, C_1, D_1, C_2, D_2, \dots, C_N, D_N]^T$
γ_1, γ_2	= pre- and post-yield stiffness ratio
$\delta(\cdot)$	= Dirac delta function
ζ	= damping ratio
ζ_g	= filter damping ratio
λ	= non-linearity strength
σ_{X0}	= standard deviation of a linear system
σ_X	= response standard deviation
ω_g	= filter frequency
ω_1, ω_2	= frequencies correspond to pre- and post-yield stiffness
ω_n	= natural frequency of a linear system
ω_n	= frequency of the n th harmonic component

Acknowledgments

This work was supported by the National Natural Science Foundation of China (Grant no. 51678464). The first author would like to thank the Chinese Scholarship Council (CSC) for financial support (File no. 201706955030) during his visit to Rice University as a visiting scholar.

Appendix. Fourier coefficient of the slowly varying term

Consider the Fourier integrals in Eq. (19)

$$U_n = \frac{2}{T_0} \int_0^{T_0} t^{-q} \cos \omega_n t dt$$

$$V_n = \frac{2}{T_0} \int_0^{T_0} t^{-q} \sin \omega_n t dt$$
(A.1)

To obtain an explicit solution for Eq. (A.1), one may invoke the corresponding Fourier transform

$$W(\omega) = \int_{-\infty}^{\infty} t^{-q} e^{-i\omega t} dt = \Gamma(1-q)(i\omega)^{q-1}$$
(A.2)

and consider the relationship between the sample values of continuous Fourier transform and discrete Fourier coefficients. That is

$$U_n = \frac{2}{T_0} \text{Re} [W(\omega_n)] = \frac{2\Gamma(1-q)}{T_0} \omega_n^{q-1} \cos \frac{\pi(q-1)}{2}$$
(A.3)

$$V_n = \frac{2}{T_0} \text{Im} [W(\omega_n)] = \frac{2\Gamma(1-q)}{T_0} \omega_n^{q-1} \sin \frac{\pi(q-1)}{2}$$
(A.4)

Numerical integration method or the Fast Fourier Transform (FFT) can also be utilized to calculate the Fourier coefficients and to validate the analytical solutions. Specifically, to avoid the instability that may be caused by the singular point $t = 0$, a numerical integration method can be developed based on

$$U_n = \lim_{\epsilon_1 \rightarrow 0} \left[\frac{2}{T_0} \left(\frac{\epsilon_1^{1-q}}{1-q} \right) + \frac{2}{T_0} \int_{\epsilon_1}^{T_0} t^{-q} \cos \omega_n t dt \right]$$
(A.5)

$$V_n = \lim_{\epsilon_2 \rightarrow 0} \frac{2}{T_0} \int_{\epsilon_2}^{T_0} t^{-q} \sin \omega_n t dt$$
(A.6)

References

- [1] J. Li, J.-B. Chen, *Stochastic Dynamics of Structures*, John Wiley & Sons, Singapore, 2009.
- [2] M. Di Paola, A. Pirrotta, A. Valenza, Visco-elastic behavior through fractional calculus: an easier method for best fitting experimental results, *Mech. Mater.* 43 (2011) 799–806.
- [3] C.G. Koh, J.M. Kelly, Application of fractional derivatives to seismic analysis of base-isolated models, *Earthq. Eng. Struct. Dyn.* 19 (1990) 229–241.
- [4] M. Sasso, G. Palmieri, D. Amodio, Application of fractional derivative models in linear viscoelastic problems, *Mech. Time-Depend. Mater.* 15 (2011) 367–387.
- [5] L. Gaul, P. Klein, S. Kempfle, Impulse response function of an oscillator with fractional derivative in damping description, *Mech. Res. Commun.* 16 (1989) 297–305.
- [6] R.L. Bagley, P.J. Torvik, Fractional calculus in the transient analysis of viscoelastically damped structures, *AIAA J.* 23 (1985) 918–925.
- [7] L.E. Suarez, A. Shokooh, An eigenvector expansion method for the solution of motion containing fractional derivatives, *J. Appl. Mech.* 64 (1997) 629–635.
- [8] M. Sasso, G. Palmieri, D. Amodio, Application of fractional derivative models in linear viscoelastic problems, *Mech. Time-Depend. Mater.* 15 (2011) 367–387.
- [9] P.D. Spanos, B.A. Zeldin, Random vibration of systems with frequency-dependent parameters or fractional derivatives, *J. Eng. Mech.-ASCE* 123 (1997) 290–292.
- [10] O.P. Agrawal, Stochastic analysis of dynamic systems containing fractional derivatives, *J. Sound Vib.* 247 (2001) 927–938.
- [11] K. Ye, L. Li, J.X. Tang, Stochastic seismic response of structures with added viscoelastic dampers modeled by fractional derivative, *Earthq. Eng. Eng. Vib.* 2 (2003) 133–139.
- [12] Z.L. Huang, X.L. Jin, C.W. Lim, Y. Wang, Statistical analysis for stochastic systems including fractional derivatives, *Nonlinear Dynam.* 59 (2010) 339–349.
- [13] L. Chen, W. Zhu, First passage failure of SDOF nonlinear oscillator with lightly fractional derivative damping under real noise excitations, *Probab. Eng. Mech.* 26 (2011) 208–214.
- [14] L. Chen, Q. Lou, Z. Li, W. Zhu, Stochastic stability of the harmonically and randomly excited duffing oscillator with damping modeled by a fractional derivative, *Sci. China-Phys. Mech. Astron.* 55 (2012) 2284–2289.
- [15] P.D. Spanos, G.I. Evangelatos, Response of a non-linear system with restoring forces governed by fractional derivatives—time domain simulation and statistical linearization solution, *Soil Dyn. Earthq. Eng.* 30 (2010) 811–821.
- [16] A. Di Matteo, I.A. Kougioumtzoglou, A. Pirrotta, P.D. Spanos, M. Di Paola, Stochastic response determination of nonlinear oscillators with fractional derivatives elements via the wiener path integral, *Probab. Eng. Mech.* 38 (2014) 127–135.
- [17] P.D. Spanos, A. Di Matteo, Y. Cheng, A. Pirrotta, J. Li, Galerkin scheme-based determination of survival probability of oscillators with fractional derivative elements, *J. Appl. Mech.* 83 (2016) 121003.
- [18] P.D. Spanos, B.A. Zeldin, Monte Carlo treatment of random fields: a broad perspective, *Appl. Mech. Rev.* 51 (1998) 219–237.
- [19] A. Shokooh, L. Suárez, A comparison of numerical methods applied to a fractional model of damping materials, *J. Vib. Control* 5 (1999) 331–354.
- [20] M.P. Singh, T.-S. Chang, H. Nandan, Algorithms for seismic analysis of MDOF systems with fractional derivatives, *Eng. Struct.* 33 (2011) 2371–2381.
- [21] P.D. Spanos, M. Di Paola, G. Failla, A Galerkin approach for power spectrum determination of nonlinear oscillators, *Meccanica* 37 (2002) 51–65.
- [22] M. Shinozuka, G. Deodatis, Simulation of stochastic processes by spectral representation, *Appl. Mech. Rev.* 44 (1991) 191–204.
- [23] H. Cramér, M.R. Leadbetter, *Stationary and related stochastic processes : sample function properties and their applications*, *J. R. Stat. Soc. A* 131 (1968) 106.
- [24] K.B. Oldham, J. Spanier, *The Fractional Calculus: Theory and Applications of Differentiation and Integration to Arbitrary Order*, Elsevier, 1974.

- [25] K. Trenevski, Z. Tomovski, On some fractional derivatives of functions of exponential type, *Publ. Elektroteh. Fak. Ser. Mat.* 13 (2002) 77–84.
- [26] R. Bouc, M. Defilippi, A Galerkin multiharmonic procedure for nonlinear multidimensional random vibration, *Internat. J. Engrg. Sci.* 25 (1987) 723–733.
- [27] P.D. Spanos, I.A. Kougioumtzoglou, C. Soize, On the determination of the power spectrum of randomly excited oscillators via stochastic averaging: an alternative perspective, *Probab. Eng. Mech.* 26 (2011) 10–15.